Serveur Académique Lausannois SERVAL serval.unil.ch

Author Manuscript
Faculty of Biology and Medicine Publication

This paper has been peer-reviewed but dos not include the final publisher proof-corrections or journal pagination.

Published in final edited form as:

serval
serveur académique lausannois

UNIL | Université de Lausanne
Faculté de biologie
et de médecine

CYSTEINE-RICH DOMAIN ONE OF CD40 MEDIATES RECEPTOR SELF-ASSEMBLY

Cristian R. Smulski[1,6], Julien Beyrath[1,6], Marion Decossas[1], Neila Chekkat[1,6], Philippe Wolff [2], Karine Gionnet[3], Gilles Guichard[3], Daniel Speiser[4], Pascal Schneider[5] and Sylvie Fournel[1,6]

[1] Institut de Biologie Moléculaire et Cellulaire, Immunologie et Chimie Thérapeutiques, CNRS UPR 9021, 15 rue René Descartes, 67084 Strasbourg, France. [2] Institut de Biologie Moléculaire et Cellulaire, Plateforme Protéomique Strasbourg Esplanade, 15 rue René Descartes, 67084 Strasbourg, France. [3] Institut Européen de Chimie et de Biologie CBMN, Université de Bordeaux I - CNRS UMR 5248; 2 Rue Robert Escarpit, 33607 PESSAC, France. [4] Department of Oncology and Ludwig Center for Cancer Research, University of Lausanne, Switzerland. [5] Department of Biochemistry, University of Lausanne, Boveresses 155, CH-1066 Epalinges, Switzerland. [6] Current addresses: JB: Centre for Systems Biology and Bioenergetics, Radboud University Nijmegen medical Centre, 6500HB, Nijmegen, The Netherlands. SF and NC: Laboratoire de Conception et Application de Molécules Bioactives, Equipe de Biovectorologie, UMR 7199 CNRS-Université de Strasbourg, Faculté de Pharmacie, 74 Route du Rhin, 67401 Illkirch, France. CRS: Department of Biochemistry, University of Lausanne, Boveresses 155, CH-1066 Epalinges, Switzerland

Running title: CRD1-mediated CD40 self assembly.

Address correspondence to either: Cristian Smulski, Department of Biochemistry, University of Lausanne, Ch. des Boveresses 155, CH-1066 Epalinges, Switzerland.
Phone +41 216925743, Fax +41 216925705 CristianRoberto.Smulski@unil.ch
or: Sylvie Fournel, Laboratoire de Conception et Application de Molécules Bioactives, Equipe de Biovectorologie, UMR 7199 CNRS-Université de Strasbourg, Faculté de Pharmacie, 74 Route du Rhin, 67401 Illkirch, France. Phone +33 368854173, Fax +33 3 68854306 s.fournel@unistra.fr

Background: The activation of CD40 is essential for the development of humoral and cellular immune responses.
Results: CD40 dimerizes through the extracellular region via the CRD1 and recombinant CRD1 potentiates CD40L activity.
Conclusion: CD40-CRD1 participates to dimerization and is required for efficient receptor expression.
Significance: CD40 self-assembly modulates signalling, possibly by maintaining the receptor in a quiescent state.

SUMARY

The activation of CD40 on B cells, macrophages and dendritic cells by its ligand CD154 (CD40L) is essential for the development of humoral and cellular immune responses. CD40L and other TNF superfamily ligands are non-covalent homotrimers, but the form under which CD40 exists in the absence of ligand remains to be elucidated. Here we show that both cell surface-expressed and soluble CD40 self-assemble, most probably as non-covalent dimers. The cysteine-rich domain 1 (CRD1) of CD40 participated to dimerization and was also required for efficient receptor expression. Modelization of a CD40 dimer allowed the identification of lysine 29 in CRD1, whose mutation decreased CD40 self-interaction without affecting expression or response to ligand. When expressed alone, recombinant CD40-CRD1 bound CD40 with a K_D of 0.6 μM. This molecule triggered expression of maturation markers on human dendritic cells and potentiated CD40L activity. These results suggest that CD40 self-assembly modulates signalling, possibly by maintaining the receptor in a quiescent state.

Ligand-induced oligomerization is an important process for activating cell-surface receptors like cytokine receptors, G-protein-coupled receptors, protein-tyrosine kinase receptors, Toll-like receptors, and tumor necrosis

factor receptor superfamily members (TNFRSF) in a number of biological events [1,2]. TNF family ligands form non-covalent homotrimers that can bind three receptor molecules [3]. Although this ligand-receptor complex is generally accepted to be the minimal requirement for signalling, some members of the family are only efficiently triggered by at least two adjacent trimeric ligands [4,5]. The form under which ligand-free TNFRSF members exist is still not fully understood. Indeed unliganded TNFR1 crystallized as a parallel dimer [6,7] while cell-based experiments rather proposed that receptors may pre-assemble as trimers in the absence of ligand [8]. Interestingly, DcR3 (TNFRSF6B) assembled as parallel dimers when crystallized alone, but as trimers when co-crystallized with its ligand TL1A, each receptor in this trimeric form contacting a different ligand [9]. Thus, receptors may exist both as dimers or trimers depending on the context. Gathering more structural information on unliganded TNF receptors will help to better understand the mechanism of ligand-induced receptor signalling.

The extracellular region of TNFRSF members is characterized by the presence of cysteine-rich domains (CRDs) which typically contain six cysteine residues engaged in the formation of three disulfide bonds. The number of CRDs in a given receptor usually varies from one to four [3]. TNFR1 and CD40 possess four CRDs, of which only CRD2 and 3 are directly involved in ligand binding. Crystallography of unliganded TNFR1 (TNFRSF1A) [6] showed homo-dimerization in either parallel or antiparallel manners [7]. Antiparallel dimers associate through an interface that overlaps with CRD1 and 2, whereas parallel dimers associate mainly via CRD1 and leave ligand binding sites accessible. Cell-based studies identified a pre-ligand-binding assembly domain at the N-terminus of TNFR1 and 2 that is required for pre-assembly of TNFR complexes in a fully ligand-responsive conformation [8]. In any case, TNF receptors appear to exist as preformed complexes and not as monomeric receptors that would only oligomerize upon ligand binding. In line with these results, the CRD1 of Fas (TNFRSF6) was shown to be essential for the formation of homotypic, ligand-independent receptor complexes [10]. The situation is more complex for the TNF-related apoptosis-inducing ligand (TRAIL), another TNF family member that

binds five different receptors: two fully functional death receptors, TRAIL-R1 (TNFRSF10A) and TRAIL-R2 (TNFRSF10B), two membrane bound "decoy" receptors, TRAIL-R3 (TNFRSF10C) and TRAIL-R4 (TNFRSF10D) and a soluble "decoy" receptor, OPG (TNFRSF11B). Decoy receptors inhibit cell death by competing for TRAIL binding. However, inhibition of TRAIL-induced apoptosis by TRAIL-R4 critically depends on its association with TRAIL-R2 via the N-terminal domain containing the first partial CRD of both receptors. Thus, in contrast to homotypic TNFR1 or Fas complexes, TRAIL-R2 and TRAIL-R4 form mixed complexes as a mean to regulate TRAIL-induced apoptosis [11].

The present study focuses on CD40 (TNFRSF5). Engagement of CD40 by CD40L leads to CD40 clustering, recruitment of TNFR associated factors and activation, among others, of the transcription factor NF-κB [12,13]. CD40 is mainly expressed on professional antigen presenting cells *i.e* dendritic cells, macrophages and B cells [14], and its activation is essential for the development of humoral and cellular immune responses. Thus, selective blockade or activation of CD40 is of pharmacological interest. The crystal structure of CD40-CD40L was recently solved showing that CRD2 and CRD3 are both involved in CD40L binding [15]; however little is known about the function of CRD1 and CRD4.

Here we show that CD40 exists as preformed, non-covalent dimers on the cell surface and that dimerization is dependent on the extracellular region. Mutation of K29 in CRD1 impaired CD40 self-assembly. Recombinant CD40-CRD1 bound the extracellular domain of CD40 with a K_D of about 0.6 μM and displayed an agonist-like activity on CD40-expressing cells such as human dendritic cells. Co-incubation of CD40-CRD1 with CD40L potentiated the NF-κB response induced by CD40L alone, suggesting that CRD1 interactions participate in CD40 signalling. These observations provide a novel mean to manipulate CD40 signalling.

EXPERIMENTAL PROCEDURES

Cell lines and reagents – Human embryonic kidney HEK293 cells were grown in RPMI 1640 medium (Lonza, Basel) supplemented with 10% fetal calf serum and 5 μg/mL of penicillin and streptomycin. Anti-CD40 (clone C20) monoclonal

antibody from Santa Cruz Biotechnology (Santa Cruz, CA) and horse radish peroxydase-coupled anti-myc antibody from Life technologies (Carlsbad, CA) were used for western blot analysis. Two different CD40L (CD154) were used as indicated: muCD8-CD40L (Ancell, MN) and Mega-CD40L (Adipogen, CA). Antibodies for flow cytometry analysis were purchased from Becton-Dickinson (Franklin Lakes, NJ): Pacific blue CD14 and PerCp5.5 HLA-DR were used for monocyte purification control; PE-Cy7 CD86, PerCp5.5 HLA-DR and APC CD83 were used to follow monocyte-derived dendritic cell maturation.

Molecular cross-linking at the cell surface - Approximately 2×10^7 HEK293 cells stably expressing CD40 or BJAB cells were washed three times with ice-cold PBS (pH 8) within the culture flask (HEK cells) or in 15 mL tubes (BJAB cells). BS^3 cross-linker (Thermo scientific, Waltham, MA) was added at a final concentration of 3 mM for 1 h at 4°C. The reaction was quenched by addition of Tris at a final concentration of 20 mM for 15 minutes. Cells were then harvested and analyzed by western blot.

Recombinant proteins - Myc-His-tagged CD40 was produced in HEK293 cells using the mammalian expression vector pSectag2-Hy (Life technologies) and purified from cell culture supernatant by nickel affinity chromatography. The encoded mature protein sequence was DAAQPAMNS, followed by amino acids 20-193 of human CD40 and the sequence QAAARGGPEQKLISEEDLNSAVDHHHHHH. The CRD1 of CD40 was expressed in *E.coli* BL21 Rosseta-gami 2 using the expression vector pET22b+ (Merck KGaA, Darmstadt, Germany). The encoded protein sequence was MDIGINSDPNS, followed by amino acids 20-62 of human CD40 and the sequence AAALEHHHHHH. Mutations K29A, K29E, C26Q or the triple mutation C37G/C38G/C41G were introduced by conventional molecular biology techniques. Bacteria were induced for production of the proteins at an OD 600 nm of 0.6 with 0.5 mM isopropyl β-D-thiogalactoside for 16 h at 20°C. Soluble periplasmic proteins were extracted and purified by nickel affinity chromatography as described in [16].

Mass spectrometry - Prior to mass analysis, protein samples were dialyzed against 200 mM ammonium acetate on Amicon Ultra-4 centrifugal filter unit-10000NMWL (Millipore, Billerica, MA). Mass spectrometry was performed on an ESI-TOF mass spectrometer Q-TOF micro (Waters, MA). Purity and homogeneity were verified by mass analysis in denaturing conditions: the protein was diluted to a concentration of 0.3 µM in water - acetonitrile (1:10, v/v) acidified with 1 % formic acid.

In non-denaturing conditions, the mass measurement of the protein was performed in 50 mM ammonium acetate with 10% isopropanol, to preserve the native conformation. The protein was injected at 2.0 µM. Clusters of Cs(n+1)In were used for the calibration of the extended masse range in the high m/z region. Mass data were acquired in the positive ion mode on the mass range 1000-10000 m/z. CD40 deglycosylation was performed using the deglycosylation mix from New England Biolabs (Ipswich, MA) following manufacturer instructions.

Molecular modelling - All procedures were performed with Discovery Studio 2.5 software from Accelrys (San Diego, CA). The crystal structure of the ligand-free TNFR1 (PDB 1NCF) was used as template to build a model of dimeric CD40. The receptor monomer correspond to the crystal structure of the complex CD40-CD40L (PDB 3QD6). A fixed atom constraint was applied to both C-terminal residues and the dimeric CD40 model was subjected to an initial minimization step (max 500), RMS gradient 0.1 kcal/mol by conjugated gradient; followed by a second minimization step (max 500), RMS gradient 0.0001 kcal/mol by conjugated gradient. The structure was then submitted to a dynamic simulation including heating (2000 steps), equilibration (1000 steps) and production (1000 steps) at 300 °K with a time step of 0.001 ps under a distance-dependent, dielectric constant, implicit solvent model. A negative intermolecular energy of -361.5 kcal/mol was obtained for the complex under these conditions. *In silico* mutation K29A produced an increase on the interaction energy to -218.0 kcal/mol, indicating a less stable complex. All images were generated using PyMOL Molecular Graphics System, Version 1.0, Schrödinger, LLC.

FRET experiments - CD40-ECFP, CD40-EYFP and the negative control ERBB2-EYFP c-terminal fusion proteins all contained the full length

receptor sequences. Mutations K29A and K29E were introduced by site directed mutagenesis. Experiments were performed using a LSRII (BD Biosciences) flow cytometer instrument. EYFP signal was recorded using the 488 nm laser with a 530/30 filter, ECFP signal was recorded using the 405 nm laser with a 450/50 filter and FRET signal was recorded using the 405 nm laser with a 585/42 filter. For each condition we evaluated a minimum of ten thousand -ECFP -EYFP double positive cells. HEK293 cells where transiently transfected with ECFP and EYFP fusion receptors and analyzed at 16 h post-transfection. Positive FRET cells were gated using an ECFP-EYFP fusion protein as positive control and a co-transfection of EFCP and EYFP as negative control according to [17].

Surface plasmon resonance - The BIACORE® 3000 system, sensor chip CM5, surfactant P20, amine coupling kit containing N-hydroxysuccinimide and N-Ethyl-N'-dimethylaminopropyl carbodiimide, and ethanolamine were from BIACORE (Uppsala, Sweden). Biosensor assays were performed with HBS-EP buffer as running buffer (10 mM HEPES, 150 mM sodium chloride, 3 mM EDTA 0.005% surfactant P20, pH 7.4). The low carboxylated dextran matrix (B1) was activated with 35 µL of a mixture 0.2 M N-ethyl-N-dimethylaminopropyl carbodiimide and 0.05 M N-hydroxysuccinimide at 5 µL/min. The anti-myc antibody (Life technologies) was immobilized with the standard BIACORE protocol at ~2000 RU per channel. Soluble CD40-myc tag fusion protein was injected for 30 sec, then increasing concentrations of recombinant CRD1 were injected for 2 min, followed by a dissociation phase of 3 min at a flow rate of 30 µL/min. All dilutions were performed in running buffer. The sensor chip surface was regenerated after each experiment by injecting 20 µL of 3 M MgCl$_2$. The kinetic parameters were calculated using the BIAeval 4.1 software. Analysis was performed using the simple Langmuir binding model. The specific binding profiles were obtained after subtracting the response signal from the control anti-myc antibody alone channel and from blank-buffer injection. The fitting to each model was judged by the chi square (χ2) value and randomness of residue distribution compared to the theoretical model. Active concentration was determined under mass transfer condition where the slope of the curves is directly correlated with the active concentration of the protein [18].

Luciferase reporter assay - HEK293 cells stably expressing either wt CD40 or CD40-K29A were cultured in 24 well plates at 3×10^5 cell/mL. After 24 h cells were transfected with control luciferase vectors or promoter specific luciferase reporter vectors (Panomics, Fremont, CA), using FuGene6 transfection reagent (Roche, Basel). Reporter luciferase assays were performed for STAT3, AP1, CRE, NF-κB and SRE that all are CD40L-activated transcription factors. After 24h, cells were treated with CD40L or a recombinant CD40-CRD1 protein at the indicated concentrations in the presence of 20 µg/mL of polymyxin B (Fluka, St. Louis, MO). After 16 h cells were lysed and luciferase activity was determined using a Wallac Victor^2 1420 multilabel counter (PerkinElmer, Waltham, MA) according to instructions of the Promega luciferase assay system. Dual luciferase assay was performed using NF-κB reporter plasmid together with renilla luciferase plasmid for normalization. Detection of firefly luciferase and renilla luciferase expression was done using the dual luciferase assay detection kit (Promega, MA).

Monocyte-derived dendritic cell differentiation and maturation - Elutriated monocytes were obtained from the Etablissement Français du Sang (EFS; Strasbourg, France). Monocytes were cultured in RPMI 1640 with Ultraglutamine (Lonza) supplemented with 10 µg/mL of gentamycin, 2 mM HEPES and 10% heat-inactivated fetal calf serum. At day 0, cells were seeded at a density of 4×10^6 cells per well in a 6-wells plate and differentiation into CD209-positive dendritic cells was induced by addition of 5 ng/mL of GM-CSF^{HuXp} and 5 ng/mL of IL-4^{HuXp} (Humanzyme, Chicago, IL). At day 5, when greater than 80% of the cells expressed CD209 (data not shown), cells were incubated with the indicated stimuli in the presence or absence of 100 µg/mL of polymyxin B (Fluka). After 24 h of culture, cells were harvested, washed with 2 mL of cold PBS and maturation maker expression was analyzed by flow cytometry.

Flow cytometry analysis - Cells were stained in PBS containing 2% fetal calf serum at 4°C for 20 min with the various antibodies used at concentration recommended by the manufacturer.

After two washes in PBS, cells were analyzed by flow cytometry with a Gallios flow cytometer (Beckman Coulter, CA). At least 10,000 events were acquired for each experiment and the data were processed with the Kaluza® Flow Analysis Software (Beckman Coulter, CA).

Statistical analysis - FRET experiments were analyzed using one-way ANOVA with Tukey post-test, luciferase NF-κB and monocyte-derived dendritic cell maturation assays were analyzed using two-way ANOVA with Bonferroni post-test; using GraphPad Prism version 5.00 for Windows, GraphPad Software, San Diego California USA, www.graphpad.com

RESULTS

CD40 dimerizes through the extracellular region - In order to define the oligomerization state of CD40 in the absence of ligand, HEK cells stably transfected with full length wt CD40 were chemically cross-linked with the non-permeable reagent BS[3]. Western blot analysis revealed that a portion of CD40, migrating at ~45 kDa, shifted to a dimer of ~90 kDa in cross-linked cell lysates (Fig. 1A). Some CD40 dimer was also observed in the B cell lymphoma BJAB cell line that expresses endogenous CD40 (Fig. 1A). To define the contribution of the extracellular region to dimerization, soluble CD40 fused to the non-oligomerizing Myc and His tags was produced in mammalian cells. This soluble CD40 bound CD154 in a surface plasmon resonance assay (data not shown). Under denaturing SDS-PAGE, soluble CD40 migrated as a band of ~36 kDa under both reducing and non-reducing conditions, but the same protein eluted with an apparent molecular weight of ~72 kDa from a size exclusion chromatography column, suggesting that it may form roughly globular dimers (Fig. 1B). Although glycosylation interfered with ionization of soluble CD40 in native mass spectrometry (Suppl. Fig. 1), the deglycosylated protein behaved well in this assay which allowed detection of two peaks at masses of 23.94 and 47.86 kDa, corresponding relatively closely to expected theoretical values for the non glycosylated monomeric (23.4 kDa) and dimeric (46.7 kDa) CD40 (Fig. 1C). Taken together, these results indicate that at least a fraction of CD40 can self-assemble in the absence of ligand, most probably as a non-covalent homodimer.

CD40-CRD1 mediates self-interaction of CD40 - In order to define the site required for CD40 self-assembly, we first constructed a model of a CD40 dimer based on the structures of the parallel TNFR1 dimer (1NCF) and ligand-bound CD40 (3QD6). The rational was that a) the structure of monomeric (liganded) and dimeric (unliganded) TNFR1 differ strongly in CRD1, suggesting that this domain is important for self-assembly (Suppl. Fig. 2A), b) lymphotoxin α-TNFR1 is the closest available crystal structure to CD40-CD40L [15], and given that c) CRD1 and 2 of TNFR1 and CD40 superimpose with a Cα root mean square deviation of 1.05 Å, chances of getting a relevant model were good (Suppl. Fig. 2B).

The model suggested the involvement of the CRD1 domain in CD40 self-assembly, with an important contribution of Lys29 (Fig. 2A). We therefore generated full-length CD40 constructs with mutation K29A, K29E or with mutations predicted to disrupt folding of the first A1 sub-domain (C26Q) or of the entire CRD1 (triple cysteine mutant C37G-C38G-C41G: mutC), or lacking CRD1 but retaining the signal peptide (CD40ΔCRD1) (Fig. 2B). With the exception of the K29A and K29E mutants, all other untagged or EYFP-tagged CD40 CRD1 mutants were all retained in the endoplasmic reticulum, failed to efficiently reach the cell surface and did not respond to exogenously added CD40L (Fig. 2C; Suppl. Fig. 3, 4 and 5A), indicating that CD40 is sensitive to mutations affecting normal folding of its CRD1. In line with these results, steered molecular dynamic simulation showed strong local perturbations in CD40-CRD1 in the case of C26Q and mutC mutations and strong local perturbations in CD40-CRD2 in the case of the delta CRD1 construct (Supp. Fig. 5B). As mentioned above, the CD40 dimer model suggested a contribution of Lys29 in receptor dimerization, and it is noteworthy that this residue is conserved in human and mouse CD40. *In silico* mutation of this residue to an alanine increased the interaction energies from -361 kcal/mol to -219 kcal/mol, highlighting its importance in receptor dimerization. We also introduced the mutation K29E in order to obtain a stronger effect by charge repulsion. Neither K29A nor K29E mutations alter the surface expression of CD40 (Fig. 2D). Furthermore, CD40L induced NF-κB activity was similar in wt CD40 cell line

when compared with the mutant cell lines K29A and K29E (Fig. 2E). Under the same conditions, no activity was observed in CD40 cell line lacking the intracellular domain (CD40-ΔICD). However, the ability of the CD40 K29A or K29E mutants to produce FRET signals with either themselves or with wt CD40 was reduced by about 50%, supporting the notion that Lys29 is involved in CRD1-mediated dimerization of CD40 (Fig. 3A). Finally, chemical cross-linking of untagged mutant or wt CD40 showed a marked reduction of dimeric species at the cell surface when using both mutant receptors in comparison with wt CD40 (Fig.3B).

Recombinant CD40-CRD1 binds to CD40 - Although the isolated CD40-CRD1 was poorly secreted in HEK cells, it was successfully produced in a prokaryotic expression system with human-compatible tRNAs and enhanced ability to form disulfide bridges. CD40-CRD1 was also expressed with the K29A, K29E and CRD1-disrupting mutations C26Q or mutC (Fig. 4A). All CRD1 molecules migrated on SDS-PAGE with an apparent molecular weight of ~16 KDa despite their theoretical molecular weight of ~8 KDa. Wild type CD40-CRD1 bound to the extracellular domain of CD40 with a K_D of 5.7 x 10^{-7} M (k_{on} 2.04 x 10^3 $M^{-1}s^{-1}$ and k_{off} 1.16 x 10^{-3} s^{-1}), as determined by surface plasmon resonance analysis, whereas no binding was detected for both cysteine mutants (Fig. 4B and Suppl. Fig. 6). These data show the importance of an adequate CRD1 folding for binding to CD40. Of note, using surface plasmon resonance, the active concentration of CD40-CRD1 was estimated to be 4.7 % of the total protein. In all experiments, the mentioned concentration of CD40-CRD1 is that of the active protein. The concentration of CRD1 mutants was estimated also as 4.7 % of the total protein although it was not possible to estimate its active fraction because there are no detectable binding to CD40.

Recombinant CD40-CRD1 induces a mild ligand-like activity and potentiates CD40L signals - As expected, an overnight stimulation of CD40-expressing cells with CD40L activated the NF-κB transcription factor and induced expression of a NF-κB luciferase reporter gene (Fig. 4C). Surprisingly, soluble CD40-CRD1 showed a weak agonistic activity on wt CD40-expressing HEK cells, but not on cells expressing CD40-K29A, CD40-K29E or CD40 lacking the intracellular domain (CD40-ΔICD) (Fig. 4C). Furthermore, wt CRD1, but not the mutants, potentiated CD40L-induced NF-κB activation by up to 2-fold, with an IC50 of about 1.5 ± 0.5 μg/ml (Fig. 4D). In line with the observation that wt CD40-CRD1 could induce NF-κB activity in cells expressing wt CD40, but not in cells expressing mutant CD40, recombinant mutant CD40-CRD1 proteins were unable to increase CD40L activity in wt CD40 HEK cells. Because the CRD1 of CD40 does not interact with CD40L in the crystallographic structure of the CD40-CD40L complex [15], we believe that the observed signal potentiation results from independent effects of CD40-CRD1 and CD40L on membrane CD40.

When human monocyte-derived dendritic cells (MDDC) from different donors were treated with increasing concentrations of wt CD40-CRD1, the surface maturation markers CD86 and HLA-DR were up-regulated (Fig. 5). This effect occurred in the presence of the LPS inhibitor polymyxin B [19], making it unlikely that it was endotoxin-mediated. Moreover, CD40-CRD1 K29E was markedly less potent than its wt counterpart at stimulating dendritic cells. Unlike CD40L, wt CD40-CRD1 taken alone failed to up-regulate the activation marker CD83, suggesting that it is less potent than CD40L (Fig. 5). When dendritic cells were treated simultaneously with wt CD40-CRD1 and CD40L, a modest potentiation of CD40L-induced activation was observed at low doses of recombinant CD40-CRD1 (Suppl. Fig. 7A and B).

Taken together, our results suggest that the CRD1 of CD40 can increase CD40-dependent signals in target cells, alone or in cooperation with CD40L.

DISCUSSION

Although it is well established that CD154 (CD40L) assembles as a trimer, not much research has been conducted on CD40 oligomerization before ligand engagement and on the potential functional effect of this oligomerization. Reports from Mourad's group suggested that CD40 at the cell surface exist as disulfide-linked dimers and that disulfide-linked homodimerization was increased by CD40L [20-22]. However, all cysteine residues in the extracellular region of CD40 and other crystallized TNFR family members are engaged in intra-chain disulfide

bridges, making it unlikely that CD40 would dimerize through inter-chain extracellular covalent bonds.

In the present study, we show that CD40 can self-assemble at the cell surface in a non covalent manner, probably as dimers. Soluble CD40 also dimerizes, suggesting that the extracellular domain plays an important role in dimer formation. In addition, *in silico* modelization and site-directed mutagenesis confirmed the role of CD40-CRD1 in receptor-receptor interactions. Until now, only TNFR1 and DcR3 have been crystallized as ligand-free receptors. TNFR1 crystallized as both parallel and anti-parallel dimers [6]. The parallel dimer was stabilized by interactions involving CRD1 and exposed fully accessible TNF binding sites in CRD2 and CRD3. In contrast, the anti-parallel dimer was stabilized by interactions involving CRD1 and CRD2 that occluded the TNF binding sites. Parallel TNFR dimers are favoured at neutral pH, while anti-parallel TNFR dimers are favoured at acidic pH [7]. This observation led to the hypothesis that parallel dimers may occur at the cell surface and could serve to create an activation network in the presence of ligand, in contrast to anti-parallel dimers that may form upon acidification of endocytic vesicles and release the ligand from the complex [7]. Unliganded DcR3 was also crystallized as parallel dimers, with the main contact area in CRD1 and 4, and an accessible ligand binding site to its ligand TL1A [9]. Sedimentation equilibrium analyses of DcR3 showed weak self-association, with an estimated equilibrium dissociation constant greater than 2.4 x 10^{-3} M, a low value if we consider that the physiological concentration of this soluble receptor is in the range of 10^{-12} pM [23]. Interestingly, the CRD1-CRD1 interaction surface modelled for CD40 in our study superimposed relatively well with the interaction surface found between the CRD1 of the TNF receptor HVEM and the immunomodulatory protein BTLA in the HVEM – BTLA complex [24]. Therefore, a CRD1 seems to use the same interface to interact with another CRD1 (as in the TNFR1 dimer) or with a regulatory protein. The CRD1 could therefore be considered as an interaction domain that regulates receptor activity by interacting either with itself or with other proteins such as BTLA.

Using surface plasmon resonance, an equilibrium dissociation constant of 5.7 x 10^{-7} M was determined for the interaction between CD40 and recombinant CD40-CRD1. Although this equilibrium constant is rather low, it may still be relevant since local protein concentrations on the cell membrane can be high, especially in some micro-domains, and since other interaction sites outside CRD1 may also participate to dimerization. These results raise the question of whether the active form of the receptor is the dimeric or the monomeric form, and whether receptor dimers persist after ligand engagement. Further analyses are warranted to address these questions.

The CRD1 of TNFR1 fused to glutathione-S-transferase as been previously described as an inhibitor of TNFR1-mediated signalling [25]. This molecule could block the effects of TNF *in vitro* and was shown to inhibit arthritis in mice [25]. Unfortunately, this study was not designed to address the molecular basis of these effects, nor did it test the potential impact of glutathione-S-transferase-induced dimerization on CRD1 activity. In the case of Fas, the study of dominant-interfering mutations associated with autoimmune lymphoproliferative syndrome (ALPS) revealed that Fas CRD1 was fully preserved in all dominant-interfering mutations, including mutations that truncate Fas after 57 or 62 amino acids of the mature Fas protein and that would be unable to bind FasL [10]. In addition, deletion of CRD1 in dominant-negative inhibitory receptors restored susceptibility to FasL-induced apoptosis, indicating that mutant proteins must physically interact with wild type proteins to create a non-functional complex. Although the phenotype of patients provide strong genetic evidence for a dominant-negative function of the N-terminal portion of Fas, results obtained with N-terminal Fas deletion mutants must be taken with caution in view of our results demonstrating that CRD1 disruption prevents CD40 surface expression. At least for CD40, N-terminal truncation or severe perturbations of CRD1 structures are not appropriate to study CRD1 function. In any case, the studies mentioned above indicate that the N-terminal portions of TNFR1 and Fas taken alone antagonize receptor signalling.

Because of the described inhibitory activity of TNFR1 and Fas CRD1, the ability of recombinant CD40-CRD1 to induce a weak CD40 activation rather than an inhibition of NF-κB signalling was

7

unexpected. A gross artefact can probably be excluded as NF-κB activation was CD40-dependent, and as CRD1 disruption mutants were ineffective. The agonist activity of CD40-CRD1 could be explained in several ways: a) if CD40 is inhibited by dimerization, then recombinant CRD1 may activate CD40 by disrupting the dimers. b) recombinant CRD1 could oligomerize CD40 on the cell surface, inducing an agonist-like signalling, and c) recombinant CRD1 may induce conformational changes in the receptor similar to those induced by the ligand upon signal activation. Importantly, the agonist activity of CD40-CRD1 was not restricted to cells overexpressing CD40, but was also observed in primary, monocyte-

derived dendritic cells. However, the observation that CD40-CRD1 was unable to induce the full set of activation markers in dendritic cells probably indicates a weak agonist activity compared to CD40L.

Altogether, our result have revealed the ability of CD40 to self-assemble through its cysteine-rich domain 1 and the ability of recombinant CD40-CRD1 to potentiate CD40L in HEK CD40 cells and to induce a ligand-like activity in human dendritic cells. Our data indicate that CD40 homo-dimerization controls signalling, possibly by maintaining the receptor in a quiescent state, although further studies are needed to elucidate mechanisms mediating receptor activation.

REFERENCES

1. Tetsch, L., and Jung, K. (2009) *Amino Acids* **37**, 467-477
2. Heldin, C. H. (1995) *Cell* **80**, 213-223
3. Bodmer, J. L., Schneider, P., and Tschopp, J. (2002) *Trends Biochem Sci* **27**, 19-26
4. Holler, N., Tardivel, A., Kovacsovics-Bankowski, M., Hertig, S., Gaide, O., Martinon, F., Tinel, A., Deperthes, D., Calderara, S., Schulthess, T., Engel, J., Schneider, P., and Tschopp, J. (2003) *Mol Cell Biol* **23**, 1428-1440
5. Haswell, L. E., Glennie, M. J., and Al-Shamkhani, A. (2001) *Eur J Immunol* **31**, 3094-3100
6. Naismith, J. H., Devine, T. Q., Brandhuber, B. J., and Sprang, S. R. (1995) *J Biol Chem* **270**, 13303-13307
7. Naismith, J. H., Devine, T. Q., Kohno, T., and Sprang, S. R. (1996) *Structure* **4**, 1251-1262
8. Chan, F. K., Chun, H. J., Zheng, L., Siegel, R. M., Bui, K. L., and Lenardo, M. J. (2000) *Science* **288**, 2351-2354
9. Zhan, C., Patskovsky, Y., Yan, Q., Li, Z., Ramagopal, U., Cheng, H., Brenowitz, M., Hui, X., Nathenson, S. G., and Almo, S. C. (2011) *Structure* **19**, 162-171
10. Siegel, R. M., Frederiksen, J. K., Zacharias, D. A., Chan, F. K., Johnson, M., Lynch, D., Tsien, R. Y., and Lenardo, M. J. (2000) *Science* **288**, 2354-2357
11. Clancy, L., Mruk, K., Archer, K., Woelfel, M., Mongkolsapaya, J., Screaton, G., Lenardo, M. J., and Chan, F. K. (2005) *Proc Natl Acad Sci U S A* **102**, 18099-18104
12. Pullen, S. S., Miller, H. G., Everdeen, D. S., Dang, T. T., Crute, J. J., and Kehry, M. R. (1998) *Biochemistry* **37**, 11836-11845
13. Pullen, S. S., Labadia, M. E., Ingraham, R. H., McWhirter, S. M., Everdeen, D. S., Alber, T., Crute, J. J., and Kehry, M. R. (1999) *Biochemistry* **38**, 10168-10177
14. van Kooten, C., and Banchereau, J. (2000) *J Leukoc Biol* **67**, 2-17
15. An, H. J., Kim, Y. J., Song, D. H., Park, B. S., Kim, H. M., Lee, J. D., Paik, S. G., Lee, J. O., and Lee, H. (2011) *J Biol Chem*
16. Smulski, C., Labovsky, V., Levy, G., Hontebeyrie, M., Hoebeke, J., and Levin, M. J. (2006) *FASEB J* **20**, 1396-1406
17. Banning, C., Votteler, J., Hoffmann, D., Koppensteiner, H., Warmer, M., Reimer, R., Kirchhoff, F., Schubert, U., Hauber, J., and Schindler, M. (2010) *PLoS One* **5**, e9344
18. Richalet-Secordel, P. M., Rauffer-Bruyere, N., Christensen, L. L., Ofenloch-Haehnle, B., Seidel, C., and Van Regenmortel, M. H. (1997) *Anal Biochem* **249**, 165-173
19. Cardoso, L. S., Araujo, M. I., Goes, A. M., Pacifico, L. G., Oliveira, R. R., and Oliveira, S. C. (2007) *Microb Cell Fact* **6**, 1

20.	Reyes-Moreno, C., Girouard, J., Lapointe, R., Darveau, A., and Mourad, W. (2004) *J Biol Chem* **279**, 7799-7806

21.	Girouard, J., Reyes-Moreno, C., Darveau, A., Akoum, A., and Mourad, W. (2005) *Mol Immunol* **42**, 773-780

22.	Reyes-Moreno, C., Sharif-Askari, E., Girouard, J., Leveille, C., Jundi, M., Akoum, A., Lapointe, R., Darveau, A., and Mourad, W. (2007) *J Biol Chem* **282**, 19473-19480

23.	Wu, Y., Han, B., Sheng, H., Lin, M., Moore, P. A., Zhang, J., and Wu, J. (2003) *Int J Cancer* **105**, 724-732

24.	Compaan, D. M., Gonzalez, L. C., Tom, I., Loyet, K. M., Eaton, D., and Hymowitz, S. G. (2005) *J Biol Chem* **280**, 39553-39561

25.	Deng, G. M., Zheng, L., Chan, F. K., and Lenardo, M. (2005) *Nat Med* **11**, 1066-1072

FIGURE LEGENDS

FIGURE 1. CD40 dimerizes through the extracellular region.
Panel A. BJAB cells and stably transfected CD40 HEK cells where treated or not with the non permeable chemical crosslinker BS[3]. CD40 was then detected by western blotting with an anti-CD40 antibody.
Panel B. The recombinant extracellular region of CD40 was analyzed by SDS-PAGE in the presence or absence of β-mercaptoethanol (left) and by size exclusion chromatography (right).
Panel C. Native mass spectrometry analysis of the recombinant extracellular region of CD40. The protein was deglycosylated before native mass analysis. The insert shows a Western blot analysis of soluble CD40 before and after deglycosylation.

FIGURE 2. CD40 CRD1 is required for normal surface expression.
Panel A. Detail of the CD40 dimer model in the region of CRD1-CRD1 interaction, showing side chains of K29, D49 and W71.
Panel B. Schematic representation of the CRD1 domain of CD40 with disulfide bridges highlighted. Mutations tested are indicated.
Panel C. Flow cytometry analysis of HEK293 cells transfected with untagged WT or mutant CD40 constructs. Staining was performed with an anti-CD40 antibody in permeabilized or non-permeabilized (surface) conditions.
Panel D. Flow cytometry analysis of different CD40-HEK293 stable cell lines used in this study. Staining was performed with Fc-CD40L followed by anti-human Fc-PE.
Panel E. Dose-response of CD40L in a NF-κB luciferase activity assay in different CD40-expressing HEK cell lines (CD40-wt, CD40-K29A, CD40-K29E and CD40-ΔICD).

FIGURE 3. Mutations of lysine 29 disrupt CD40 self-assembly.

Panel A. Cytometric FRET analysis of CD40 interaction with either wt CD40, CD40-K29A or CD40-K29E, using both ECFP and EYFP fusion combinations. ($p<0.01$, **).

Panel B. CD40 stable cell lines (wt, K29A and K29E) were treated or not with the non permeable chemical crosslinker BS^3. CD40 was then detected by western bloting with an anti-CD40 antibody. Densitometry analysis is shown on the right as a ratio between monomeric and dimeric receptors. NS: non-specific signal.

FIGURE 4. Recombinant CD40-CRD1 binds to CD40 and potentiates CD40L activity.

Panel A. Purified CD40-CRD1, CRD1-K29E, CRD1-K29A, CRD1-C6Q and CRD1-mutC (20 µg protein/lane) were resolved by SDS-PAGE and stained with Coomasie blue.

Panel B. Biacore sensorgram of CD40-CRD1 binding to the entire extracellular domain of CD40.

Panel C. Luciferase reporter assay for NF-κB activity in different CD40 HEK cell lines (CD40-wt, CD40-K29A, CD40-K29E and CD40-ΔICD) treated with recombinant soluble CD40-CRD1. Untreated cells are shown on the left and Mega-CD40L stimulated cells are shown on the right.

Panel D. Luciferase reporter NF-κB assay in HEK CD40 cell line treated with 500 ng/ml of CD40L and increasing concentrations of recombinant soluble CD40-CRD1, CRD1-K29A, CRD1-K29E, CRD1-C6Q and CRD1-mutC. ($p<0.05$, *; $p<0.01$, **; $p<0.001$, ***).

FIGURE 5. Recombinant CD40-CRD1 induces maturation of human monocyte-derived dendritic cells.

Panel A. CD14 positive cells (scattergram on the left) were cultured in the presence of IL-4 and GM-CSF for 5 days. Cells were then treated for 24 h with PBS (Vehicle), LPS (10 µg/mL) or LPS plus polymyxin B (100 µg/mL) (LPS+PMX) and analyzed for expression of activation markers CD86 and HLA-DR on CD209 positive cells.

Panel B. Expression of maturation markers CD86, HLA-DR and CD83 (geo-mean, gMFI) was assessed after treatment with the indicated concentrations of recombinant wt CD40-CRD1 or CD40-CRD1 K29E in the presence of polymyxin B (100 µg/mL). Control treatments CD40L (200 ng/mL of Mega-CD40L) and LPS plus polymyxin B (100 µg/mL) (LPS+PMX) are also shown for each donor. Mean value with SEM of triplicates are shown ($p<0.001$, ***). Data is representative of two independent experiments performed on a total of three different donors.

Figure 1
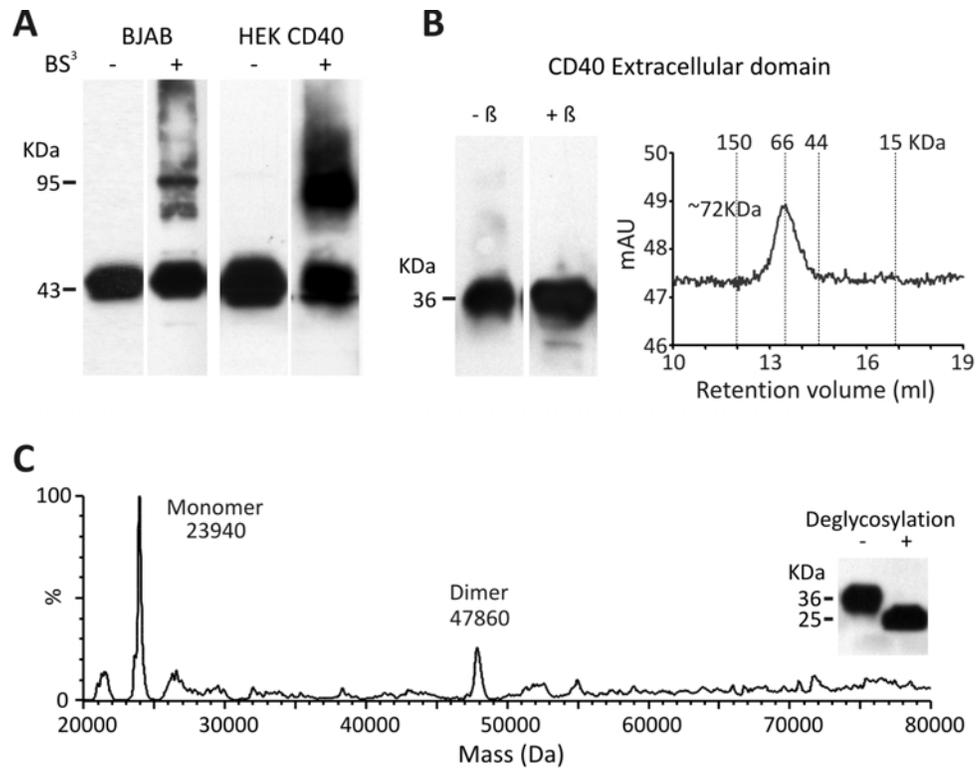
Figure 2
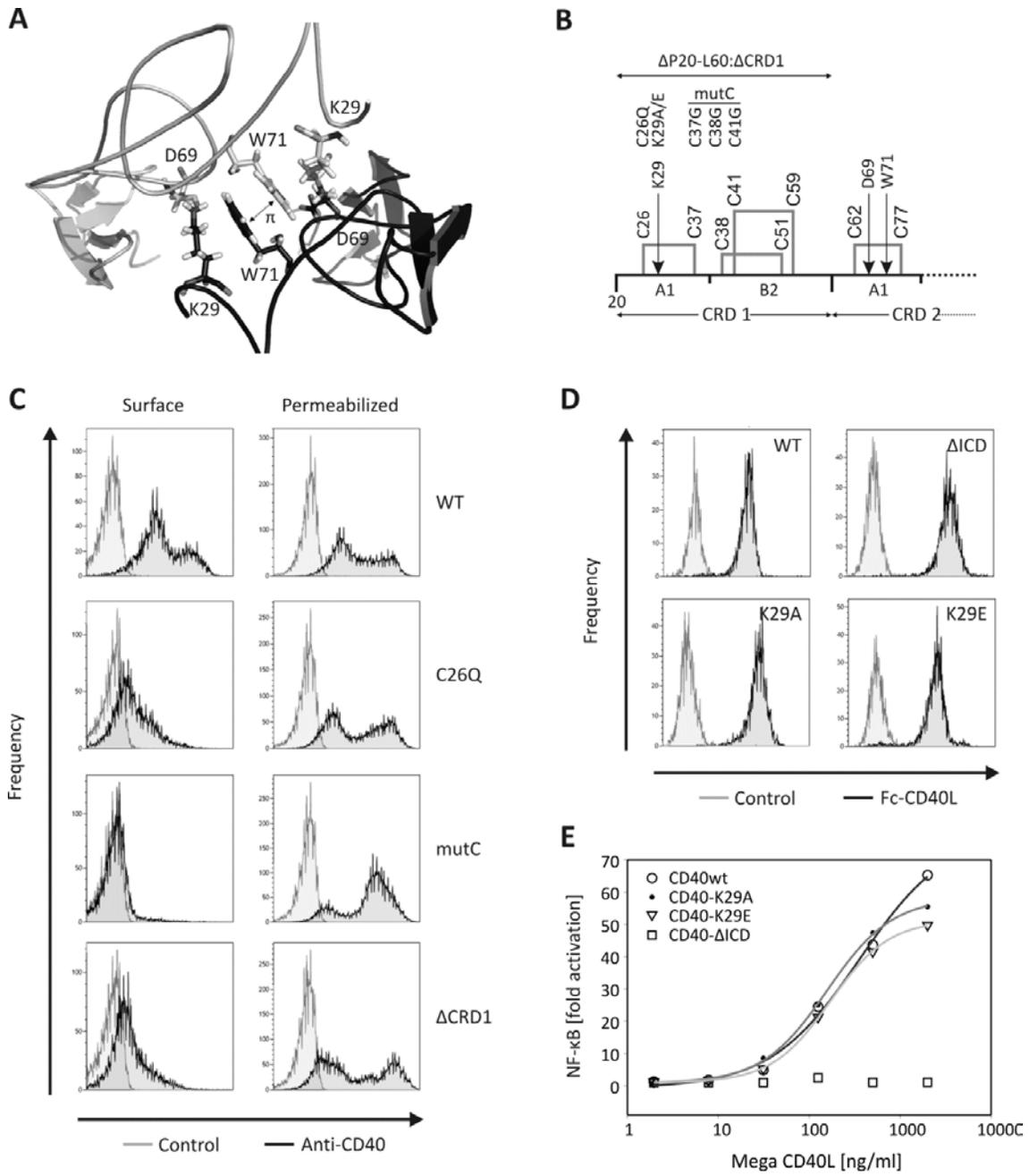
Figure 3

Figure 4

Figure 5